Journal of Medicinal Chemistry

Subscriber access provided by American Chemical Society

Article

Mapping Antimalarial Pharmacophores as a Useful Tool for the Rapid Discovery of Drugs Effective in Vivo: Design, Construction, Characterization, and Pharmacology of Metaquine

Michael J. Dascombe, Michael G. B. Drew, Harry Morris, Prapon Wilairat, Saranya Auparakkitanon, Wendy A. Moule, Said Alizadeh-Shekalgourabi, Philip G. Evans, Michael Lloyd, Anthony M. Dyas, Pamela Carr, and Fyaz M. D. Ismail

J. Med. Chem., **2005**, 48 (17), 5423-5436• DOI: 10.1021/jm0408013 • Publication Date (Web): 26 July 2005

Downloaded from http://pubs.acs.org on March 28, 2009

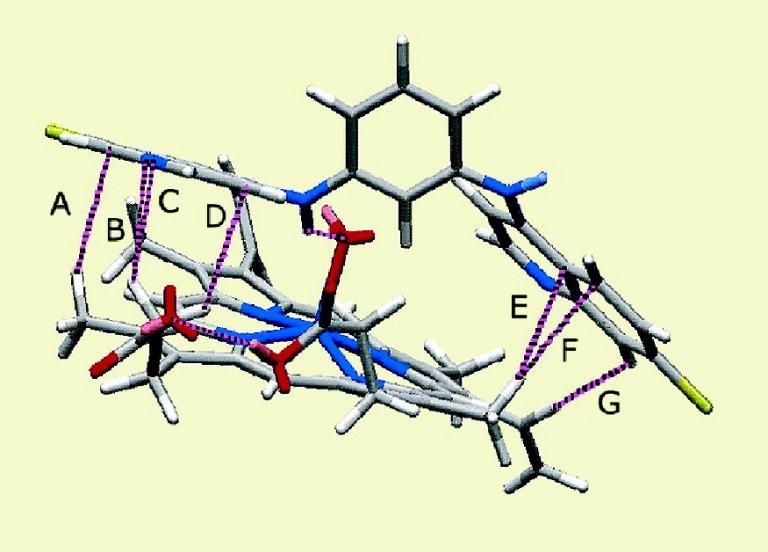

More About This Article

Additional resources and features associated with this article are available within the HTML version:

- Supporting Information
- Links to the 4 articles that cite this article, as of the time of this article download
- Access to high resolution figures
- Links to articles and content related to this article
- Copyright permission to reproduce figures and/or text from this article

View the Full Text HTML

ACS Publications
High quality. High impact.

Journal of Medicinal Chemistry is published by the American Chemical Society. 1155 Sixteenth Street N.W., Washington, DC 20036

Articles

Mapping Antimalarial Pharmacophores as a Useful Tool for the Rapid Discovery of Drugs Effective in Vivo: Design, Construction, Characterization, and Pharmacology of Metaquine

Michael J. Dascombe,[*,†,⊥] Michael G. B. Drew,[*,‡,⊥] Harry Morris,[§] Prapon Wilairat,[#] Saranya Auparakkitanon,[#] Wendy A. Moule,[§,||] Said Alizadeh-Shekalgourabi,[§,||] Philip G. Evans,[‡,§] Michael Lloyd,[§] Anthony M. Dyas,[§] Pamela Carr,[||] and Fyaz M. D. Ismail[*,§,⊥]

Faculty of Life Sciences, Stopford Building 1.124, The University of Manchester, Oxford Road, Manchester M13 9PT, U.K., School of Chemistry, University of Reading, Reading RG6 6AD, U.K., The Medicinal Chemistry Research Group, The School of Pharmacy and Chemistry, Liverpool John Moores University, Liverpool L3 3AF, U.K., Faculty of Science, Department of Biochemistry, Mahidol University, Bangkok 10400, Thailand, and Department of Chemistry, University of Hertfordshire, Hatfield AL10 9AB, U.K.

Received March 2, 2004

Resistant strains of *Plasmodium falciparum* and the unavailability of useful antimalarial vaccines reinforce the need to develop new efficacious antimalarials. This study details a pharmacophore model that has been used to identify a potent, soluble, orally bioavailable antimalarial bisquinoline, metaquine (*N,N′*-bis(7-chloroquinolin-4-yl)benzene-1,3-diamine) (dihydrochloride), which is active against *Plasmodium berghei* in vivo (oral ID_{50} of 25 μmol/kg) and multidrug-resistant *Plasmodium falciparum* K1 in vitro (0.17 μM). Metaquine shows strong affinity for the putative antimalarial receptor, heme at pH 7.4 in aqueous DMSO. Both crystallographic analyses and quantum mechanical calculations (HF/6-31+G*) reveal important regions of protonation and bonding thought to persist at parasitic vacuolar pH concordant with our receptor model. Formation of drug−heme adduct in solution was confirmed using high-resolution positive ion electrospray mass spectrometry. Metaquine showed strong binding with the receptor in a 1:1 ratio ($\log K = 5.7 \pm 0.1$) that was predicted by molecular mechanics calculations. This study illustrates a rational multidisciplinary approach for the development of new 4-aminoquinoline antimalarials, with efficacy superior to chloroquine, based on the use of a pharmacophore model.

Introduction

Rational design of novel antimalarial drug candidates, with the consequent reduction in screening costs, may provide an efficient contribution, if not solution, to the much needed decrease in the disease burden of malaria.[1] Hemoglobin proteolysis by intraerythrocytic malaria parasites releases both oxygen radicals and heme (Fe(III)PPIX, Figure 1a) that are detoxified by dismutation and biomineralization, respectively. At acidic pH, heme biomineralization occurring in the feeding vacuole of *Plasmodium* is inhibited in the presence of chloroquine (Figure 1b), subsequently allowing production of a redox active peroxidation catalyst.[2a] Quinoline antimalarials may act by preventing sequestration of this toxic heme into hemozoin,[2b] promoting oxidative stress that can lead to parasite death.[2c] The concentration of free hemin is rigorously regulated in the vertebrate host by a circulating, high-affinity ($K_d < 1 \times 10^{-12}$ M) plasma protein, hemopexin, which is catabolized in liver cells.[2d] Heme has been implicated as the main receptor for 4-aminoquinoline antimalarials. It exists in a monomeric form at acidic pH and as the μ-oxo dimer at basic pH.[3] Although the stoichiometry and spectroscopic characteristics of drug−heme binding are known,[3] "the structures of hematin−aminoquinoline complexes are unknown, and so the steric and electronic requirements for inhibition of β-hematin formation are likely to be difficult to establish".[4] In the absence of crystallographic detail, computational modeling of drug−receptor complexes is a suitable approach for improving rational drug design of 4-aminoquinoline antimalarials.[3] In this study, we report a pharmacophore model for 4-aminoquinoline antimalarials that can be used to select compounds from commercial or, as in this case, in-house libraries for further investigation as potentially useful clinical drugs.

Results and Discussion

Structural and Modeling Studies. Over the past 20 years we have critically evaluated numerous established and novel custom-designed analogues of mono-

* To whom correspondence should be addressed. For M.J.D.: phone, +44 (0)161 275 5353; fax, +44 (0)161 275 5363; e-mail, mike.dascombe@manchester.ac.uk. For M.G.B.D.: phone, +44 (0)118 378 8789; fax, +44 (0)118 378 6331; e-mail, m.g.b.drew@reading.ac.uk. For F.M.D.I.: phone, +44 (0)151 231 2231; fax, +44 (0)151 231 2170; e-mail, f.m.Ismail@livjm.ac.uk.

⊥ These authors have contributed equally to this study.

† The University of Manchester.

‡ University of Reading.

§ Liverpool John Moores University.

Mahidol University.

|| University of Hertfordshire.

10.1021/jm0408013 CCC: $30.25 © 2005 American Chemical Society
Published on Web 07/26/2005

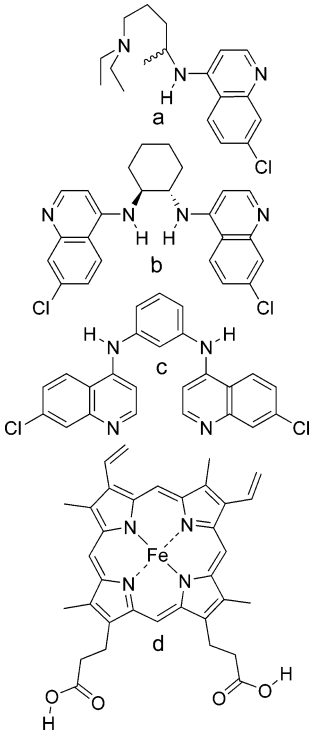

Figure 1. Structures of (a) chloroquine, (b) Ro 47-7737, (c) metaquine, and (d) heme.

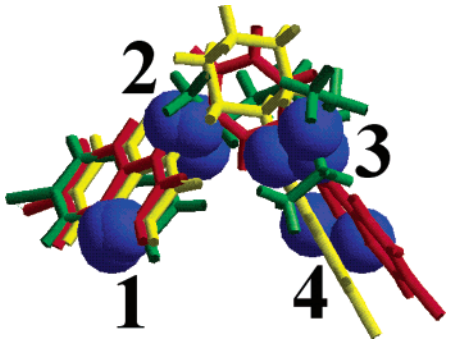

Figure 2. Biophoric map of selected quinolines, acridines, and bisquinolines. Regions 1 and 4 are proton acceptors. In all 110 apex biophore maps generated, regions 1 and 4 were hydrogen atom donors and regions 3 and 4 were hydrogen atom acceptors. Consequently, the preferred site(s) of protonation in metaquine is(are) the endocyclic quinoline nitrogen(s) (compare with Ro 47-7737).[13d]

and bis-4-aminoquinolines,[5,6] artemisinins, pyrimethamine,[7a] peroxides,[7b] dinitroanilines,[8] and 9-aminoarylacridines and benznaphthyridines[9] in order to correlate molecular structures with antimalarial activity in vivo, thereby identifying the antimalarial pharmacophore functional in vivo for each class of compound. Using 4-aminoquinolines (e.g., chloroquine, Figure 1b; Ro 47-7737, Figure 1c), 9-aminoarylacridines and benznaphthyridines of varying potency, this study defines a minimum functional pharmacophore in vivo for these antimalarials (Figure 2) in a *Plasmodium berghei* model of malaria.[5] Key features of this pharmacophore, revealed by APEX modeling[10] (Figure 2), are consistent with published structure−activity relationships, including the dimensions of preferred intramolecular N−N distances.[5,6,11,12] Importantly, chloroquine, which was excluded from the training set, was predicted to be active in vivo. Several novel substances from our in-

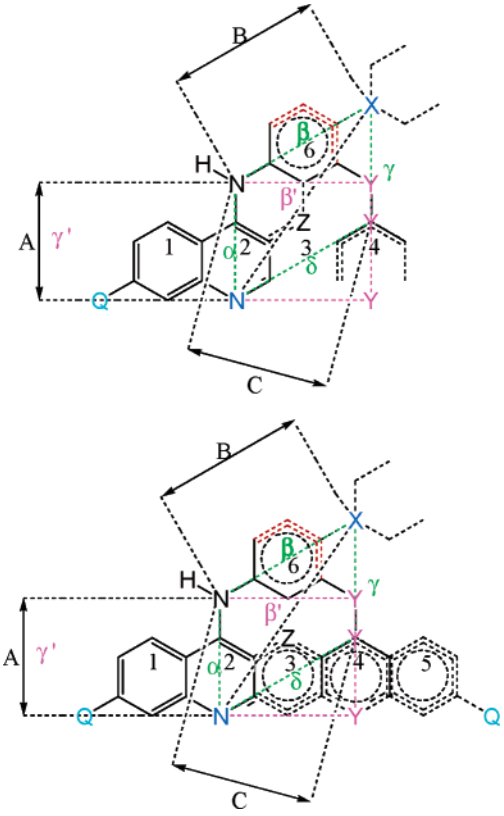

Figure 3. (a) Aminoquinoline pharmacophore (upper graphic). When Y = OH, then substituent 4 is absent and X = N and dotted lines linked to X are ethyl, piperidinyl, or pyrrolidinyl groups. β is aromatic when red portion is present and is aliphatic when it is absent. Q = CF_3, H, F, Br, Cl, or I. (b) Bisquinoline pharmacophore (lower graphic). When ring 3 is absent, then Z designates a hydroxyl group if attached to ring α or methyl group if attached to ring denoted β. If ring 3 is present, it is fused to the b vertex of either ring 2 or 4. In ring 4, Y = N or CH (which results in loss of drug potency). For example, this pharmacophore has led to the prediction that the meta isomer of amodiaquine, 5-(7-chloroquinolin-4-ylamino)-2-diethylaminomethylphenol (SN-13,730), will be more potent than the parent compound (Ismail et al. Unpublished study; see also ref 31a,b). In the most active analogues, ring 3 is absent as are substituents on X on ring β. The bridging unit can be aromatic or cycloalkyl. See refs 5, 6, and 13 for leading examples including Ro 47-7737.

house drug bank of over 60 000 compounds, as well as the bisquinoline Ro 47-7737 (Figure 1c),[13] were predicted by this pharmacophore model (Figure 2) to be highly active. These selected compounds were assayed for antimalarial activity both in vivo against lethal *Plasmodium berghei* in mice and in vitro against drug-resistant human *Plasmodium falciparum*. The compounds were also evaluated for their acute toxicity, formulation characteristics, and suitability for parenteral and oral delivery systems.

In general, our maps of the antimalarial pharmacophore(s) fall into two categories, both suggesting that drugs, especially 4-aminoquinolines and 9-aminoacridines, need to contain three or four nitrogen atoms[9] for high activity against *P. berghei* in mice (Figure 3). Various linear sequences of atoms containing only the carbon and nitrogen framework were used to query available databases, including Beilstein Crossfire, which resulted in several interesting "hits" including heme (Figure 1a).[14a] Speculating that heme-processing en-

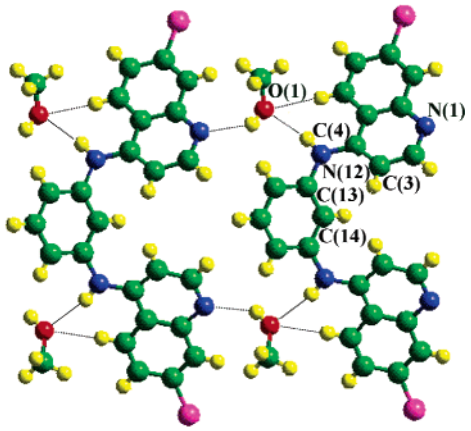

Figure 4. Crystal structure of metaquine·2MeOH: carbon, green; chlorine, purple; oxygen, red; hydrogen, yellow; nitrogen, blue. Hydrogen bonds are shown as dotted lines.

zymes[14b] or heme, released by the catabolism of host hemoglobin during malarial infection, could potentially bind such drugs, we initiated a lead directed program of drug development. This strategy produced various symmetrical bis-quinolines bridged by both flexible and rigid spacers. The latter compounds facilitated modeling experiments by decreasing the number of solution-state conformers, thus acting as useful probes for our "functional receptor".[5,6]

With this approach, a highly potent, nontoxic antimalarial drug *N,N′*-bis(7-chloroquinolin-4-yl)benzene-1,3-diamine[6] (named for convenience by us as metaquine, Figure 1d) has been discovered, which, as this study shows, is water-soluble and orally active in infected mice and is also effective against human drug-resistant malaria in vitro. Importantly, this compound is inexpensive to produce because it utilizes a key intermediate, 4,7-dichloroquinoline, already used in the manufacture of chloroquine.

The crystal structure of metaquine·2MeOH[6] is shown in Figure 4. The metaquine molecule contains a crystallographic mirror plane. The two torsion angles of note are C(3)−C(4)−N(12)−C(13) τ_1 and C(4)−N(12)−C(13)−C(14) τ_2, which are 12.9(9)° and 38.6(9)°. There are also two strong hydrogen bonds to the two solvent methanol molecules: O(1)−N(12), 2.92 Å, and O(1)−N(1), 2.73 Å. In addition, there is a weak contact with C(3)−H (O(1)···H, 2.39 Å). Figure 4 is a view down the short "*a*" axis of 4.039 Å; thus, all the aromatic rings in the structure form π stacks.

Metaquine is a relatively rigid molecule, particularly when compared to chloroquine, having only four rotatable torsion angles (τ_1−τ_4). We have carried out a conformational analysis adopting the grid search method varying these four torsion angles utilizing molecular mechanics via the Cerius[2] software[15] and obtained six low-energy conformations. These were then subjected to geometry optimization at the HF/6-31+G* level using the Gaussian 98 program.[16] The two lowest energy conformations had energies that differed by less than 0.1 kcal mol^{-1} (0.4 kJ mol^{-1}) and were 2 kcal mol^{-1} (8 kJ mol^{-1}) lower in energy than any other conformation. In these structures, the geometry was C_2 (τ_1 = 20.2, τ_2 = 41.4) and C_s (τ_1 = 20.6, τ_2 = 44.1), respectively, with the latter set of torsion angles being equivalent to that observed in the crystal structure. For example, we have shown by NMR experiments (data not shown) that the preferred sites of protonation of Ro 47-7737 are the endocyclic nitrogen atoms rather than the 4-amino groups. This is consistent with the preferred site of protonation in our mapped pharmacophore (Figures 2 and 3)[17] and as identified in an X-ray crystallographic study.[13d] Calculations were also carried out to investigate the two possible sites for protonation. The proton was added to either N(1) or N(12), and conformational analysis was conducted as above (Figure 4). For each position of the proton, the five lowest energy conformations were then subjected to geometry optimization at the HF/6-31+G* level. The lowest energy structure with N(1) protonated was lower in energy than that with N(12) protonated by 42 kcal mol^{-1} (176 kJ mol^{-1}), which confirms the former unequivocally as the preferred site of protonation. This approach of mapping the functional antimalarial pharmacophore(s) is further vindicated by the identification of five new drug candidates, which may be suitable for commercial exploitation.[18]

Second-generation pharmacophores are currently being mapped for compounds showing activity against both drug-sensitive and drug-resistant *Plasmodium* both in vitro and in vivo to validate compounds encoded by the maps presented here (Figure 3). Importantly, several binding modes of metaquine to monomeric heme have been predicted by molecular modeling using a modified MM2 force field especially parametrized for iron (Figure 5).[15]

Heme−Metaquine Modeling. Parasite catabolism of one molecule of hemoglobin releases four porphyrins from their protective protein coat. These porphyrins are rapidly oxidized to the ferric form and subsequently react with hydroxyl ions to form hematin or with chloride ions to form hemin chloride, ions that accumulate within the *Plasmodial* food vacuole.[19a,b] Parasite catabolism of hemoglobin can generate either one of these five coordinate porphyrins, which can act potentially as a receptor for 4-aminoquinoline antimalarials accumulating within this compartment.

Interactions of Quinolines with Hematin. Hydroxyl ions axially ligate hemin to form a high-spin five-coordinate complex.[20] Modeling studies involving 4-aminoquinolines and porphyrins invariably depict heme−drug interactions as a face-to-face π−π alignment, a scenario supported by interpretation of NMR data.[21] Typical aromatic−aromatic π-stacking interactions are considered weak (2 kJ mol^{-1} (quantum mechanical calculation).[22a,b] Failure to detect such interactions in our high-resolution electrospray mass spectrometry experiments between hematin and a variety of quinolines, including metaquine, suggests that such interactions are too weak to survive in the gas phase (not shown).

Automated docking interactions between metaquine and heme, using a modified MM2 method (similar to the structural decomposition engine of Shelnutt et al.[23]), generated various geometries (A−N) with similar energies (Figure 5). The lowest energy complex (Figure S1 in Supporting Information, which is the same as the table of contents graphic), which is about 10 kJ mol^{-1} lower in energy than the remaining structures, is not a face-to-face π−π alignment but one that involves a more intimate interaction that results in porphyrin ring

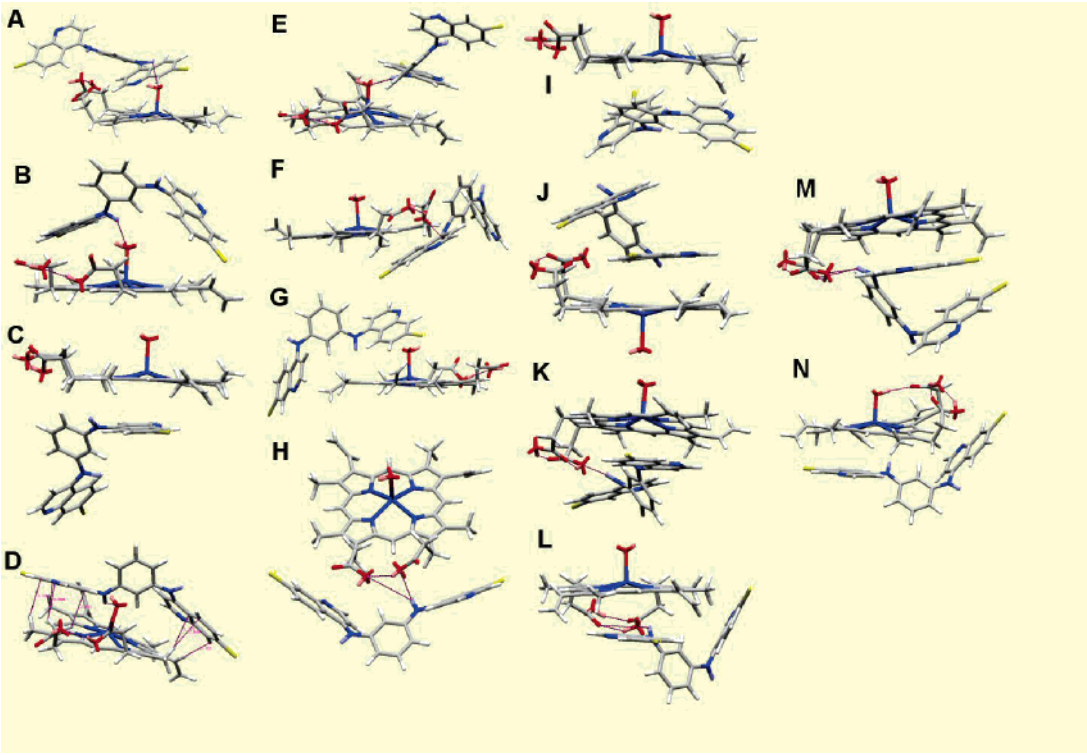

Figure 5. Interactions of hematin with metaquine, where carbon = gray, oxygen = red, nitrogen = blue, chlorine = yellow. Drug−receptor complexes can be classified as "above face" (A, B, D, E) in which the metaquine is hydrogen-bonded to the axial hydroxyl group, as "below face" (C, I−M where $\pi-\pi$ interactions are dominant, and having ring edge interactions (F−H. Structure D reveals close contacts with the heme receptor. Strongest interactions are shown as dotted lines that include CH_3 (heme)$-\pi$ (metaquine) interactions and a hydrogen bond between the carboxylate of heme and the NH group of metaquine.

deformation (ruffling).[23] A parallel-displaced interaction such as this has a significant contribution from $\pi-\sigma$ attraction, as well as van der Waals interactions This structure was obtained from manual docking followed by molecular mechanics minimization. The remaining structures depicted in Figure 5 were established by a combination of manual docking and automated Monte Carlo methods following molecular mechanics minimization. A necessary feature of the minimization process was the provision for the heme ring to become significantly nonplanar.[24c,d] For instance, binding can be either above or below the mean plane of the heme ring system (Figure 5).[24c]

NMR analyses of drug−porphyrin complexes[21] can be reinterpreted as emanating from various conformations. In contrast, geometrical analyses involving $\pi-\pi$ stacking in metal complexes with aromatic nitrogen-containing ligands confirm, based on X-ray data, that a face-to-face $\pi-\pi$ alignment, where most of the ring-plane area overlaps, is a rare phenomenon.[24] The common π interaction detected in X-ray data is an offset or slipped stacking; i.e., the rings are parallel-displaced. The ring normal and the vector between the ring centroids form an angle of about 20° up to centroid−centroid distances of 3.8 Å. Importantly, only a limited number of structures with a near-to-perfect facial alignment exists in available databases.[24a] Instances in which metal−ligand complexes involve rings−edge interactions are best described as a C−H$\cdots\pi$ attraction (e.g., Figure 5F−H).

These modeling experiments reveal close contact between various portions of the quinoline ring and heme (depicted as dotted lines in Figure 5D; see also Supporting Information Figure S1). This observation suggests that bulky substitutions at one or more of these positions will prove to be dystherapeutic. Conversely, incorporation of suitable substituents may be used to reinforce drug−receptor interactions and allow design of compounds with enhanced potency. The dominant interaction between the 7-chloroquinolinolyl substituents with the heme receptor has been suggested to be a $\pi-\pi$ or charge-transfer interaction reinforced by an ionic interaction.[5,9c] Our molecular mechanics study reveals that a linear relationship exists between the total energy of the various conformers and the sum of the van der Waals and electrostatic energy terms, implying that both contribute to the binding of metaquine with heme.

In conclusion, this part of the study confirms that our modeling approach is valid and is concordant with results obtained by the structural decomposition approach of Shelnut et al.[23] The close contacts revealed by this model afford additional opportunities for modulating drug−heme interactions. This outlines a clear strategy in which modification of close interactions between drug and receptor will form the basis of future investigations.

Interaction of Quinoline with Hemin Chloride. In competition with hemin formation, hemin chloride may also be formed during the parasite catabolism of hemoglobin. In the presence of this displaceable axial chlorine ligand, high-resolution electrospray experiments suggest that a strong bond forms, probably between the endocyclic quinoline ring nitrogen and the metal center in hemin, that survives into the gas phase (Figure 6; see also Supporting Information Figure S2). Since accumulation of high concentrations of 4-amino-

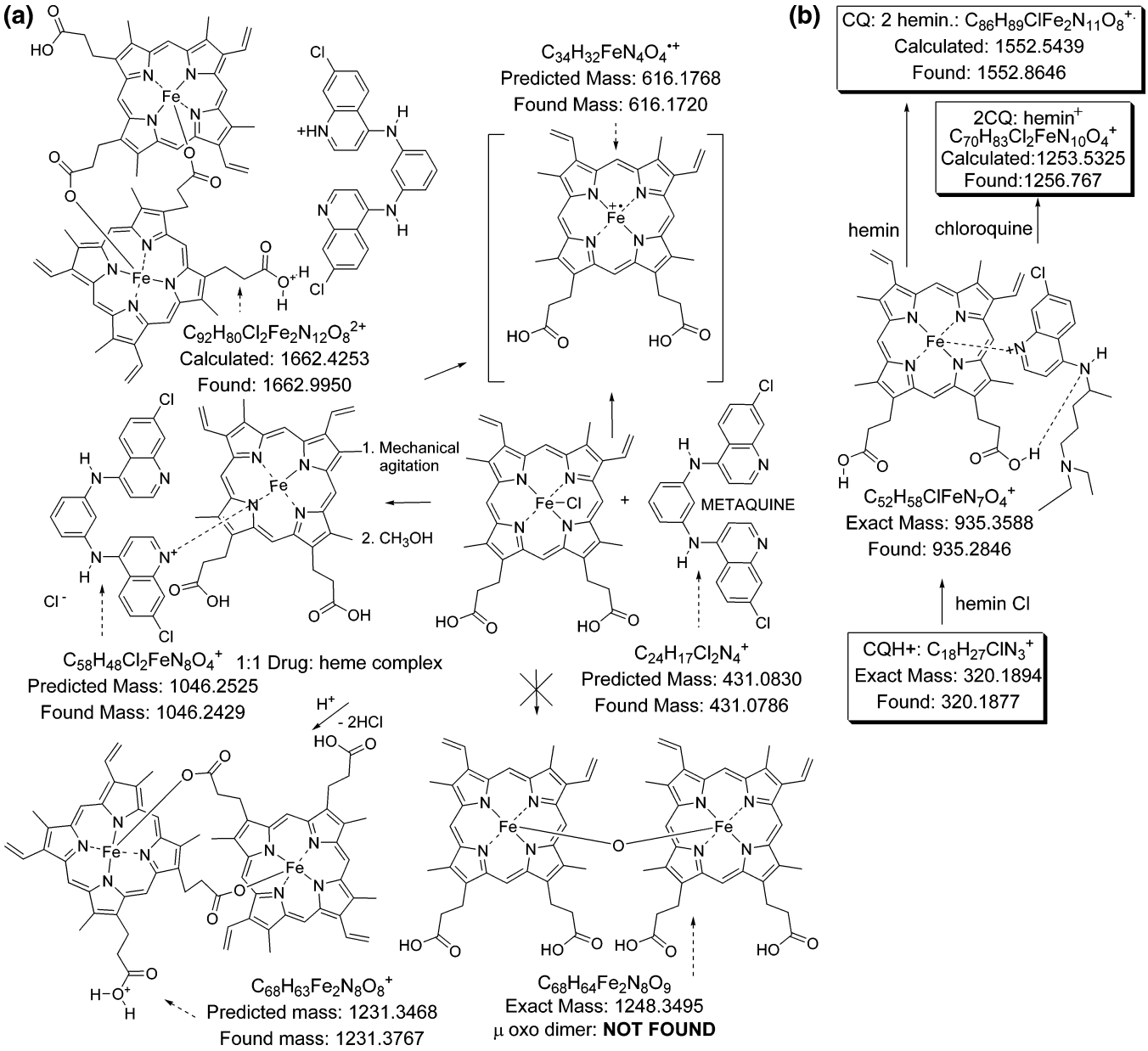

Figure 6. (a) Suggested identity of mass ions detected in positive ion electrospray mass spectra associated with mechanochemically synthesized metaquine heme complexes. (b) Suggested identity of mass ions detected in positive ion electrospray mass spectra associated with mechanochemically synthesized chloroquine heme complexes.

quinolines in the food vacuole of drug-sensitive parasites will make such a reaction pseudo-first-order, it was considered worthy of investigation by both modeling experiments and mass spectrometry studies. It is relevant and noteworthy that there is only one example in the Cambridge Crystallographic Database[25] of a crystal structure of a benzimidazole or similar ligand bound to a transition metal encapsulated in a porphyrin in the metal, although there are several examples of 2-methylimidazole complexes in axial positions. No doubt the reason for this is a significant steric interaction between the axial ligand and the porphyrin.

To investigate the viability of a quinoline ring binding in an axial site, we built such a complex and used DFT methods to assess its structure. The geometry-optimized structure is shown in Figure 7. The fold observed in the porphyrin is not excessive compared to those observed in crystal structures, but it is significant. After removing the quinoline ring, we carried out a single-point calculation on the Fe(porphyrin) structure and obtained an energy 93.7 kcal mol^{-1} (392 kJ mol^{-1}) higher than

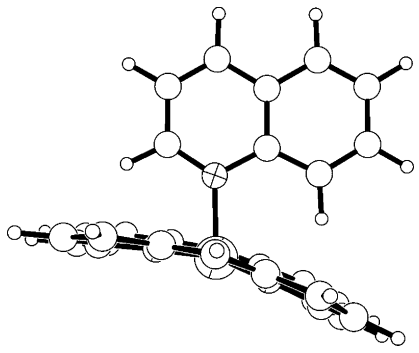

Figure 7. Geometry-optimized structure of Fe(porphyrin)-(quinoline) showing the necessary distortion fold (from the average mean plane) in the porphyrin plane due to steric effects of the hydrogen in the 2 position.

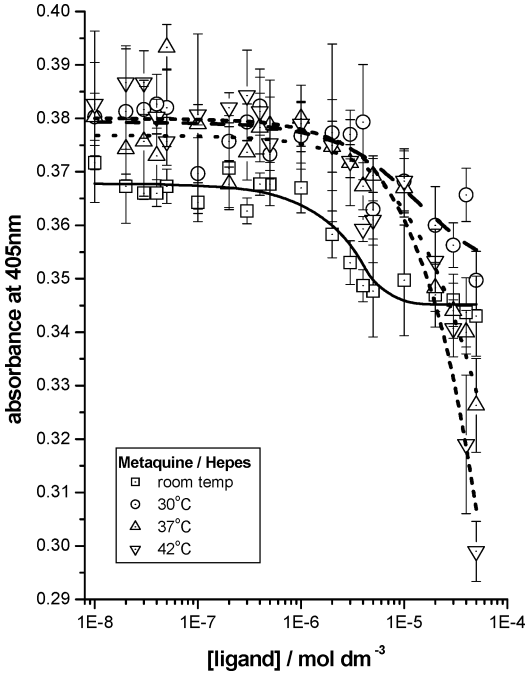

Figure 8. Drug binding studies to putative receptor (hematin). Nonlinear least-squares fitting of metaquine−heme titrations[28b,d] at room temperature (23.5 °C), 37 °C, and 42 °C.

obtained with a planar porphyrin. The remaining atoms in metaquine will not add to the close steric contacts with the prophyrin ring observed in this model structure. Such distortion can allow 4-aminoquinolines that possess a substituent at the 7 position to bind in this fashion but precludes those with halogens on the 8 position. This could be one explanation of the lack of antimalarial activity in 8-susbtituted 4-aminoquinolines.[26]

Quantifying Hematin−Drug Interactions. Avoiding the expense of a radiolabeled hematin biomineralization assay,[27,28] automation of a published monomeric heme binding assay in buffered DMSO (pH 7.4)[28b] has allowed us, by the use of microtiter plates, to screen many compounds rapidly to quantify drug−receptor interactions (Figure 8; see Supporting Information for Figure S5). From these data, calculation of binding constants (log K)[28b,e] shows that metaquine (Figure 8) has a binding constant superior to that of chloroquine (log $K = 5.7 \pm 0.1$ and 4.8 ± 0.1, respectively, 23.5 °C, which correlates with its rank ordered activity against *P. falciparum* K1 in vitro and *P. berghei* in vivo (for chloroquine hematin titration, see Figure S5 in Supporting Information). The excellent agreement between our binding constants for chloroquine (Table 1) and those of Egan et al.[28b] provides confidence that this system can be transferred to a high-throughput mode.

UV Spectra of Donor−Acceptor Complexes. Changes in the Soret band depend on pH, polarity of the solvent, and the nature of the ligand interacting with the porphyrin. Parts a and b of Figure 9 reveal

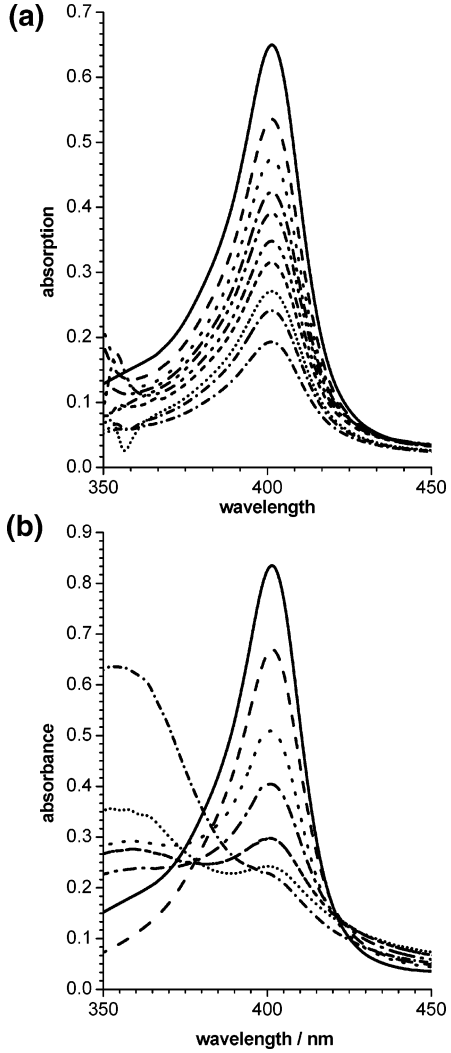

Figure 9. (a) Spectroscopic changes in the Soret band observed when hematin is titrated with increasing concentrations of chloroquine. Titration of the reference cell contents with chloroquine allows removal of any interfering bands in the UV spectrum of hematin (apparent pH 7.5, 25 °C, 40% DMSO, 0.020 M HEPES buffer). Spectra have been corrected for dilution. (b) Spectroscopic changes in the Soret band observed when hematin is titrated with increasing concentrations of metaquine. Titration of the reference cell contents with metaquine allows removal of any interfering bands in the UV spectrum of hematin (apparent pH 7.5, 25 °C, 40% DMSO, 0.020 M HEPES buffer). Spectra have been corrected for dilution.

the spectral changes within the Soret band of the electromagnetic spectrum observed when hematin is titrated with chloroquine and metaquine, respectively. Decreases in the Soret band are attributed to donor−acceptor complex formation between the hematin and 4-aminoquinoline under investigation. All experiments were conducted with homogeneous solutions obeying Beer's law. Importantly, solutions did not scatter light at the concentration studied, a result consistent with the absence of aggregate formation, i.e., hemozoin. The

Table 1. Summary of Binding Data and Thermodynamic Parameters at an Apparent pH of 7.4 (HEPES Buffer)

quinoline compd	log K (23 °C)	log K (30 °C)	log K (37 °C)	log K (42 °C)	ΔH, kJ mol^{-1}	ΔG, kJ mol^{-1}	ΔS, J K^{-1} mol^{-1}
chloroquine (K1)	5.5	5.4	5.4	5.3	−18.8	−31.2	41.8
metaquine (K1)	6.1	5.4	5.1	5.8	−15.4	−38.2	63.3

absence of any detectable precipitate and the lack of associated mass ions, when solutions were examined in high-resolution electrospray experiments, indicate the formation of donor−acceptor complexes. Aggregates are normally associated with red-shifted bands in the visible region of the electromagnetic spectrum; these were not seen in this study. The shifts detected in the UV spectra (Figure 9) of such complexes may be consequences of such an interaction causing nonplanarity in the heme.[23]

Metaquine (Figure 9b) demonstrates behavior that is more complex than chloroquine (Figure 9a). In this molecule, the presence of a bridging aromatic phenylenediamine unit allows conjugation across all three rings systems, which markedly affects the spectrum of this molecule when it interacts with the axially ligated porphyrin (see Figure 7). Therefore, methods were developed to remove this interfering absorption by the use of suitable reference solutions in reference wells on each microtiter plate.

The binding experiments are consistent with a model in which stepwise binding of hematin to either chloroquine or metaquine gives the best fit. Concordance with the 1:1 binding (heme−drug) model proposed Egan et al.[28b] suggests that this same phenomenon, observed in thermostated cuvettes, can be reliably extended to a 96-well plate system. Hence, acquisition of a large number of binding constants will allow greater definition of the steric, electronic, and lipophilic requirements of the hematin receptor.

The magnitudes of the binding constants of chloroquine (3.5×10^{-9} M [28g]) in purely aqueous systems are lower than found in the current study or that of Egan,[28b,d] since the conditions reported by Fitch favor μ-oxo dimer formation.[28g] Therefore, our measurements have been performed in a solvent system that maintains the porphyrin in a monomeric state.

Thermodynamic analyses of chloroquine−hematin and metaquine−hematin association (van't Hoff plots) in aqueous 40% DMSO suggest that both processes are entropically driven (Table 1) and show a thermodynamic compensation phenomenon consistent with the results observed for chloroquine and amodiaquine as reported by Egan et al.[28b,d] Recently, Egan and Ncokazi[28d] have highlighted the importance of water demonstrating that hydrophobic interactions are vital in stabilizing 4-aminoquinoline−hematin interactions. Our resonance Raman experiments probing associations between hematin and metaquine complement these observations reinforcing the important role of water in enforcing drug−receptor interactions.[13e] Since interactions between the 4-aminoquinolines and the receptor are weakened or nonexistent in organic solvents such as benzene,[29] translocation of 4-aminoquinoline−hematin complexes to the interior of membranes, where the dielectric constant (ϵ) is similar to that of organic solvents such as benzene ($\epsilon = 2.3$), suggests a release mechanism that allows chloroquine to shuttle back and forth between the parasitic vacuole and sites of oxidative stress within the membrane.

Evaluation of Binding Constants at Physiologically Relevant Temperatures. Many studies of a chemical nature are conducted at "room temperature", usually 20−24 °C. The ligands (chloroquine, metaquine) studied here have biological relevance in homeothermic mammalian hosts, i.e., people with body temperatures of ∼37 °C. In addition, malaria is a pyrogenic infection that can raise body temperatures in patients to 42 °C. It is appropriate, therefore, to ascertain the effects of those different temperatures on the drug target interactions (Figure 8; see Supporting Information Figure S5 for chloroquine data).

The apparent association constant (see Table 1) between chloroquine and hematin remains unchanged with increasing temperature, suggesting that chloroquine will maintain its therapeutic effect during episodes of fever. In contrast, there is a step change suggesting a decreased affinity by metaquine for hematin between room temperature and physiologically relevant temperatures.[28h] Despite this decrease in drug−receptor affinity, it remains similar to chloroquine and coupled with its activity against resistant clones of *Plasmodia* suggests that this compound is worthy of further investigation.

Mass Spectrometry of Metaquine−Hemin Adducts. It has been suggested by some researchers that complex formation between the μ-oxo dimer of hemin and various 4-aminoquinolines explains their antimalarial activity.[30] This proposal has been challenged by Egan et al.[28] who have shown that binding occurs with monomeric heme under the acidic conditions found in the feeding vacuole of *Plasmodium*. Therefore, a model system with hemin chloride in wet methanol was employed in this study. Under these apparently acidic conditions, the absence of any significant ion at 1248.3495 Da (corresponding to the hemin μ-oxo dimer; see Figure 6) suggests that drug binding in this system occurs with monomeric heme.[30b] In addition, it is possible that the high concentration of chloride ions in the parasitic vacuole could encourage formation of hemin chloride during catabolism of hemoglobin during the intraerythrocytic stage of *Plasmodium* infections. Therefore, we have investigated the reaction of metaquine with hemin chloride (Figure 6a).

Poor solubility of many potential drugs in common solvents (e.g., water, DMSO) limits their chemical analysis and biological screening. This can be overcome for 4-aminoquinoline antimalarials by studying adduct formation in the solid state. Direct mechanical agitation of salts of 4-aminoquinoline antimalarials with hemin chloride forms adducts that can then be dissolved in protic solvents and unequivocally identified by high-resolution electrospray mass spectrometry. Analysis of hemin−metaquine dihydrochloride and hemin−chloroquine phosphate adducts formed in the solid state by mechanical agitation (mechanochemical synthesis) showed complex formation similar to that seen in solution-state experiments. Reaction of a solution of hemin chloride in methanol yielded a strong molecular ion at 616.1720 Da, interpreted here as the radical cation resulting from the loss of chloride from hemin found in complexes involving chloroquine (Figure 6b) but not metaquine (Figure 6a, showing detailed interpretations of positive mass ions detected in these experiments). Hemozoin dimer subunit formation was detected (1231.3767 Da, Figure 6a), which is consistent with the structural motif present in hemozoin in the solid state.[2b] Binding of metaquine to the centrosymmetric subunit of hemozoin (1662.9950, Figure 6a and

Supporting Information Figure S2a) contradicts the suggestion by Buller et al.[28i] that metaquine does not bind in the same fashion as chloroquine, which favors binding drugs to hemozoin in edge type interactions (see Figure 5F−H). Occasionally, a small amount of a protonated hemin trimer (1851.2192 Da) was also evident (not shown), suggesting further polymerization of heme can occur in this system, especially upon storage. Similar experiments with chloroquine also showed 1:1 drug−heme adduct formation (935.2846 Da) (Supporting Information Figure S2b) and also 2:1 adduct formation (1254.3767 Da) (Supporting Information Figure S2c,d).

In the experiments reported here, the stoichiometric ratio of drug to receptor was determined more accurately (Figure 6 and Supporting Information Figure S2) than previously reported using mass spectrometry,[17g,32] NMR both in solution[33] and the solid state,[34] or calorimetry.[35] The presence of hemin enhances the solubility of the drug, which may be important in facilitating translocation of the hemin−drug complex from the acidic vacuole to the site of oxidative stress, exerted by hemin, within *Plasmodium*.[36]

Consistent with our mass spectrometry findings, quantum mechanical (QM) experiments (Figure 7) also indicate that coordination between the metal center and the drug may be favored at the endocyclic nitrogen in 4-aminoquinolines such as metaquine. Recently, it has been suggested by NMR experiments that in the solid state the iron atom within heme can coordinate to chloroquine,[34] but the data presented here are thought to be the first report of such mechanochemically synthesized bisquinoline−heme adducts analyzed by accurate electrospray mass spectrometry (Figure 6a).

Absence of Heme−μ-Oxo Dimer in Mass Spectral Studies. Hemin chloride is monomeric in the crystalline state.[37] In freshly prepared methanolic solutions, as used in this study, mass spectral analysis (Supporting Information, Figure S4) indicated that the hemin chloride remained unaltered, i.e., monomeric solution and not reacting with methanol during the time scale of the experiment. However, centrosymmetric dimerization was observed when solutions were allowed to age at room temperature or the ionic strength was changed.[38]

Linear dimeric hematins (porphyrin−*O*-porphyrin, i.e., μ-oxo dimers) possess a unique antisymmetric stretch (around 850 cm^{-1}), which was not detected in control experiments (FT-IR data not shown). Rigorous drying of solid hematin results in extensive dimer formation, which could also be occurring during the desalting procedure described by Konig et al.,[17g] but their decision to conduct experiments at pH 7.0 probably accounts for their observed mass spectra. The common practice of dissolving hemin in alkaline solutions also promotes the formation of μ-oxo dimers. Even in the solid state, porphyrins can absorb oxygen to form dimers,[39] a phenomenon preceded by the formation of a peroxyhemin complex (648.2020 Da, (see Figure S4 in Supporting Information). Hence, it is essential to prepare and investigate such drug complexes rapidly.

Antimalarial Activity of Metaquine in Vivo and in Vitro. The antimalarial activity of metaquine dihydrochloride against *P. berghei* N/13 has been previously published (ID_{50} = 2.4 μmol/kg).[6] In this study, metaquine free base displayed a similar potency against this parasite when injected sc 3−4 h after infection on day 1, then twice daily on days 2 and 3 (ID_{50} = 1.5 μmol /kg). This result shows that the relatively "insoluble" (aqueous) free base of metaquine is bioavailable from the site of oil injection. These drugs were administered in 96% olive oil with 4% DMSO, which was used as a general purpose, depot-type vehicle. In this vehicle, the ID_{50} values for metaquine, both as free base or as salt, compare favorably with that of chloroquine diphosphate (ID_{50} = 8.3 μmol/kg).

Metaquine dihydrochloride is soluble in aqueous solutions containing a small quantity (2−4%) of DMSO and, in this study, had an ID_{50} of 2.9 μmol/kg when 0.9% saline and DMSO (96:4) was used as vehicle for sc injections in *P. berghei* N/13 infected mice. Metaquine dihydrochloride was also active against a second strain of lethal rodent malaria, *P. berghei* NY in vivo (ID_{50} = 3.2 μmol/kg), when injected ip in Water for Injections BP and DMSO (96:4). Again, the activity of metaquine compared favorably with that of chloroquine diphosphate in this vehicle (ID_{50} < 4 μmol/kg).

Oral administration of drugs is usually preferred for drugs used clinically, but attempts to dissolve metaquine hydrochloride in tap water for administration in the drinking water of mice resulted in a visible precipitate, presumed to be the calcium salt(s) of the drug. Consequently the drug was dissolved in Water for Injections BP with DMSO (98:2). Drug solutions at concentrations of 65 and 199 μM were made available to *P. berghei* infected mice ad libitum for drinking. Measurement of the total volumes imbibed daily facilitated calculation of an average ID_{50} for metaquine dihydrochloride by the oral route: 25 μmol/kg.

No signs of toxicity in vivo were observed in mice for metaquine at any dose or by any route of administration used in these experiments. However, further investigations of possible toxicity, including chronic toxicities and phototoxicities, are needed.[13c−e] Preliminary experiments show metaquine does not generate singlet oxygen in SDS micelles[13e] and may not be phototoxic as speculated by Zeigler et al.[3i].

Metaquine dihydrochloride was also active against multidrug resistance human malaria (*P.* falciparum K1) in vitro. Using the technique of [^{3}H]-hypoxanthine incorporation,[40a] the IC_{50} value for metaquine was 0.17 μM, which was superior to the value for chloroquine (0.23 μM)[40b,c] in our experiments.

Conclusion

In conclusion, mapping of antimalarial pharmacophores has facilitated the design and selection of suitable compounds for both in vitro and in vivo screening of antimalarial activity. Rational selection of lead compounds results in decreased use of animals in drug evaluation while providing absolute (numeric) quantification of drug−receptor interactions. In this study, UV titrimetry in microtiter plates and electrospray mass spectrometry both confirmed that complex formation between heme and metaquine utilizes only one quinoline ring. This result, previously suggested by docking experiments, confirms that monomeric heme exists in both the solution and solid states and is able to complex 4-aminoquinolines in a quantifiable fashion. High-

throughput screening using microplate-based heme binding assay, as used here, will expedite drug development further. Obtaining a much larger set of compounds will facilitate formulation of improved pharmacophore maps.

Experimental Section

Materials and Equipment. Chloroquine diphosphate, hemin chloride, HEPES (*N*-2-hydroxyethylpiperazine-*N*′-2−ethanesulfonic acid), and spectrosol or AR grade DMSO were purchased from Sigma. Hipersolv HPLC grade water (pH 6.85) was mandatory (BDH). The Multiskan Ascent microplate reader (model 354, 405 nm filter) was purchased from Thermo Labsystems. Cliniplate and Microplate 96-well flat-bottom microtiter plates (catalog no. 9502227) or "Labsystems Microplate" (catalog no. 9502227) were purchased from Thermo Labsystems (P.O. Box 28, Helsinki, Finland). A Fisherbrand variable (20−300 μL) multifin pipet was used to load the 96-well microplates. A Hilsonic ultrasound sonicator (Hilbre Ultrasonics Ltd., England) was used to assist dissolution of substances. A pH meter 7010 (Electronic Instruments Ltd.) enabled determination of solution pH. UV spectra were acquired using a Hewlett Packard diode array spectrophotometer (model 8452A) using quartz cuvettes (1 cm, Q 10000). Data were curve-fitted using the "Origin" software package (Aston Scientific, Buckinghamshire, U.K.). Expected mass ions were calculated using CS ChemDraw Ultra 7.0.1 (Cambridgesoft Corporation, MA).

Metaquine dihydrochloride was synthesized by a published method.[6] The free base was produced by refluxing the material in concentrated ammonia (10 M), filtered, and washed until the washings became neutral. Metaquine·2HCl, 100 g, was refluxed in pyridine (2.5 L) under argon for 12 h. The solution was filtered hot through a pad of charcoal under reduced pressure and left to cool. An amount of 25 mL of this solution was placed in a desiccator containing anhydrous methanol (double-diffusion method), producing fiber-like strands over a period of 6 months. Crystal data: metaquine, MeOH, $C_{26}H_{24}Cl_2N_4O_2$, M = 495.39 Da, monoclinic, space group $P2_1/m$, a = 4.0390(8) Å, b = 32.391(10) Å, c = 8.932(3) Å, β = 90.490(18)°, U = 1168.5(6) Å^3, Z = 2, d_{calc} = 1.408 M g^{-3}. The 10 626 reflections were collected at room temperature on an Enraf/Nonius four-circle diffractometer of which 2193 were unique. The structure was solved by direct methods and refined on F^2 using Shelxl:[16b,c] R1 and wR2 are 0.0749 and 0.1281, respectively, for data with $I > 2\sigma(I)$ [41] (see Supporting Information).

Molecular Modeling Experiments. Molecular modeling was initially carried using Macromodel (Schrödinger, San Diego, CA) and Cerius[2] (version 3.5, Accelrys Inc., San Diego, CA).

Experimental Methods Involving Quantum Mechanical Calculations. The ADF program[42] was used for model structures containing transition metals. For all elements the ZORA approximation was used together with the default TZP basis sets using a small core. In addition, Vosko, Wilk, and Nusair's local exchange correlation potential was employed[43] together with Becke's nonlocal exchange[44] and Perdew's correlation corrections.[45a,b]

Washing of Glass Apparatus. Glassware was washed thoroughly before preparation of reaction solutions to ensure that no impurities affected the reaction mixture or influenced the ionizing species present. All containers were washed thoroughly with sufficient distilled water prepared by reverse osmosis. This was performed at least three times before subsequent washing with 1 M sulfuric acid, followed by a three further washes with purified water. Finally, the glassware was rinsed with Hipersolv HPLC grade water to minimize the effects of varying ionic levels on heme. It should be noted that failure to observe these protocols adversely affects the test outcome by causing aggregation of hematin, which leads to erroneous data most likely arising from changes in the ionic strength and/or salt formation. All experiments were conducted in an analytical, air-conditioned clean room environment.

Calibration of Equipment. Hipersolv HPLC grade water was tested daily to ensure that the pH did not deviate from the desired range on storage. The Sartorious electronic balance, accurate to 5 decimal places for weights under 30 g, was calibrated daily to prevent measuring and subsequent batch errors. The multichannel variable pipet was calibrated as detailed in the user's manual for 50 and 300 μL, attaining accuracy and standard deviations within the acceptable range. The pH meter was calibrated daily using the appropriate standard solutions at pH 7.0 and pH 4.0.

Preparation of Buffer Solutions. The 0.2 and 0.02 M HEPES buffer solutions were prepared by dissolving 2.3820 and 0.2382 g, respectively, accurately determined, in 50 mL of Hipersolv HPLC grade water. Buffer pH was adjusted to 7.4 using 1 and 0.1 M NaOH, respectively. MES buffer solutions, 0.2 and 0.02 M, were prepared via the same method by adjustment to pH 5.6. NaOH solutions (0.4 M) were utilized for MES pH adjustment. The mass of MES used was 2.1320 and 0.2132 g, producing end buffer solutions of 0.2 and 0.02 M, respectively, when dissolved in 50 mL of Hipersolv HPLC grade water.

Preparation of NaOH Solutions for pH Adjustment. Sodium hydroxide solutions were used to adjust the pH of the designated HEPES and MES buffer solutions. The 1 and 0.1 M stock solutions were prepared by dissolving 4.000 and 0.4000 g, respectively, of AnalaR NaOH pellets, accurately determined, in 100 mL of Hipersolv HPLC grade water. Similarly, 0.4 M solutions were prepared by dissolving 1.6 g of NaOH pellets in 100 mL of HPLC grade Hipersolv water.

Preparation of Hemin Stock Solutions. Hemin stock solutions were prepared regularly by dissolving 7−8 mg of hemin chloride (MW = 652.0), accurately determined, in 10 mL of AR grade DMSO, producing a resultant concentration of 1.2 mM. To prevent degradation and precipitation, all hemin stock solutions were stored in the dark away form UV light at 4 °C.

Preparation of Aqueous Hematin DMSO (40%) Solutions (Apparent pH 7.5). During this investigation, drug−heme interactions and respective molecular binding ratios were cross-validated using chloroquine using the aqueous DMSO assay outlined by Egan et al.[28b] in which quinoline−receptor is determined to involve hematin in the monomeric form. A clean room environment was used to run the assay to prevent undesired aggregation of hematin. Aqueous DMSO (40%) solutions of hematin were prepared daily to prevent precipitation and aggregation of the porphyrin. Solutions were prepared by dissolving 0.5 mL of hemin stock solution in 5 mL of 0.2 M HEPES buffer and 20 mL AR grade DMSO and made up to 50 mL with pure HPLC grade water. Thus, the concentration of hematin in the resultant solutions was approximately 12 μM, accurately determined for each batch. Prior to aqueous hemin preparation, stock hemin solutions were heated in a water bath at 37 °C to ensure that the uniform solubility was maintained. The resultant 40% DMSO solutions maintain hematin in the monomeric state at the concentrations used,[28b,d] allowing accurate and valid conclusions to be drawn from the data. Prepared daily, the solutions were stored in the dark at 4 °C because the compounds are photosensitive.

Preparation of Diluent Solutions. Diluent solutions were required to produce the desired concentration range for each 4-aminoquinoline. For UV analysis, blank titrations were attained using solutions constant to both heme and quinoline reagents. Diluent solutions were prepared by dissolving 10 mL of 0.02 M HEPES and 40 mL of spectroscopic grade DMSO (for monomeric hematin) and made up to a final volume of 100 mL with ultrapure, HPLC grade Hipersolv water.

Standard UV Spectrophotometric Assessment. Solutions of heme were titrated against quinoline solutions to indicate binding, if any, to heme in the aqueous hemin solution. Quartz cuvettes were initially washed with ethanol; subsequent washes with distilled water were performed after

each titration. Dilution factor corrections were not required because individually titrated solutions were used for each measurement.

UV Spectrophotometric Analysis (Apparent pH 7.4) Using the Multiskan Ascent Microplate Reader. The Multiskan Ascent microplate reader was programmed in accordance with the Ascent manual to initiate the following assay step sequence: shake (10 s), shake (10 s), pause (10 s), measure (approximately 8 s are required to scan the 96 microplate wells), display results, save to disk, export to and ascent software files, and analyze with the Origin mathematical package.

Preparation of Chloroquine Solutions. Chloroquine solutions, at an apparent pH of 7.5, were prepared by dissolving 0.257 95 g (MW = 257.95) of the diphosphate salt, accurately measured, in 5 mL of 0.02 M HEPES buffer solution and 20 mL of aqueous AR grade DMSO and made up to 50 mL with HPLC grade Hipersolv water to produce a final chloroquine concentration of 0.01 M. Once prepared, the stock solution was stirred using a hot plate and magnetic stirrer at an incubation temperature of approximately 43°C for 2 h. For the purpose of UV spectroscopic assessment, chloroquine concentrations were prepared by 1 in 10 serial dilution of 5 mL of chloroquine stock solution with 20 mL of AR grade DMSO and 5 mL of 0.02M HEPES buffer solution and made up to 50 mL with HPLC grade water. This gave final solutions of 0.001, 0.0001, and 0.000 01 M. Once prepared, all solutions were kept in the dark because chloroquine is particularly prone to photodegradation (see UV-Induced Heme Degradation).

Assay of Quinoline−Heme Interactions. Drug and diluent solutions were added to the photometric microplate as described above. The plates were then covered in a plastic plate sealer film to prevent evaporation and shaken via the plate reader for 10 s to aid mixing of the solutions. Plates were then incubated at the desired temperature (at 28, 37, or 42 °C) for 30 min. Heme solutions were also incubated at the same temperature for the same period of time in the incubation chamber. After incubation, heme was added to the 96-well plate using the Fisherbrand multichannel variable pipet. The microtiter plates were then read via the Multiskan Ascent photometric microplate, and the absorbance data were recorded for analysis.

Assay of Chloroquine−Heme Interactions. Chloroquine solutions were added to the photometric 96-well flat-bottom microplate via a Fisherbrand multichannel variable pipet. Each well had 100 μL of 12 μM heme added with the exception of two reference columns in each row. Here, 100 μL of heme was replaced with 100 μL of diluent allowing subtraction of any quinoline absorbance at each corresponding dilution. The first row acts as a blank having diluent present only, where as row 2 quantifies the absorption of heme without chloroquine.

Preparation of Metaquine Solutions. Metaquine (dihydrochloride salt MW = 504.24; free base = 431.32 Da) solutions, at an apparent pH of 7.5, were prepared by dissolving 5.0424 g of the dihydrochloride salt, accurately determined, in 5 mL of 0.02 M HEPES buffer solution and 20 mL of aqueous AR grade DMSO and made up to 50 mL with pure water prepared by reverse osmosis to produce a final metaquine concentration of approximately 0.0001 M, accurately determined for each stock solution. In cases where the free base was used the method was as above, but used 4.31 mg of the solid. However, the solubility of metaquine free base was poor (at room temperature), and this necessitated the use of the more soluble dihydrochloride salt of metaquine. Once prepared, the stock solution was stirred using a hot plate and magnetic stirrer at an incubation temperature of approximately 43°C for 6 h. It was necessary to sonicate the stock solution after incubation to ensure complete solubalization. For the purpose of UV spectroscopic measurements, metaquine concentrations were prepared by 1 in 10 serial dilution of 5 mL of metaquine stock solution with 20 mL of AR grade DMSO and 5 mL of 0.02M HEPES buffer solution and made up to 50 mL with HPLC grade water. This gave final solution concentrations of 1×10^{-5}, 1×10^{-6}, and 1×10^{-7} M. Once prepared, all solutions were kept in the dark to prevent photodegradation (see UV-Induced Heme Degradation).

Assay of Metaquine−Heme Interactions. Metaquine solutions were added to the photometric 96-well flat-bottom microplate via a multichannel variable autopipet. Each well has 100 μL of 12 μM heme added with the exception of two reference columns selected in each row. Here, 100 μL of heme was replaced with 100 μL of diluent, allowing subtraction of metaquine absorbance at each corresponding dilution. The first row acts as a blank having diluent present only. The second row indicates the absorption of heme without metaquine. Absorbance was measured at 405 nm.

Sonication of Solutions. Sonication (Hilsonic ultrasonic sonicator) was employed to aid dissolution of metaquine stock solutions and to disrupt observed aggregates of heme. Solutions were clamped in the water bath 3 cm above the ultrasonic node for a period of 30 min. A small quantity of SDS was added to the water bath to improve the sonication efficiency.

UV-Induced Heme Degradation. Heme photosensitivity was investigated using a Camag UV lamp (catalog no. 0229230). The 12 μM heme solutions were exposed to the lamp at 366 nm for 100 min with a constant distance of 36 mm maintained between the plate surface and the UV lamp (254 nm irradiation). During photodegradation experiments, microtiter plates were sealed with an acetate film to prevent solvent evaporation. The film was removed before each UV assessment and subsequently replaced after analysis. All measurements were performed in the Ascent Multiskan plate reader using eight samples for reproducibility.

Time-Dependent Decomposition of Heme. The absorbance of 100 μL of 12 μM heme solutions, diluted with 100 μL of diluent for a final heme concentration of 6 μM, was assessed at hourly intervals for a period of 10 h to determine the effect of time on heme absorbance. The plate was sealed between each UV reading to prevent evaporation of solution from the microtiter wells. Results indicate that solutions should be used within 24 h and stored in the dark until required for use.

Time-Dependent Absorbance of Heme and Quinolines in 96-Well Microtiter Plates. The assay procedure was performed in accordance with the assay procedure for chloroquine. After UV irradiation analysis, the plate was sealed to prevent evaporation and reanalyzed at 10 min intervals to a period of 1 h with the initial reading being $t = 0$. Results indicated that solutions should be freshly prepared and measured within 30 min to maximize accuracy.

Data Analysis and Mathematical Assessment. All absorbance data were attained as an average of triplicate results, allowing identification of accuracy, reproducibility, and removal of any extensive outliers in the data (principally caused by dust particles falling into a well). Various methods were utilized for analysis of UV data and fitting to binding algorithms indicating various stoichiometries between heme and the quinoline.[28b,d] Excel spreadsheets were utilized for standard optimization of the model. Excel Solver for Microsoft Windows was also utilized for assessing 1:1 binding. For standard nonlinear least-squares analysis, Origin and SPSS statistical packages were used. A computational program was devised, written in Fortran code to model and assess the fit for specific binding algorithms utilizing a Nutcracker method.

Assay of Antimalarial Activity. (a) In Vivo. *P. berghei* N/13 or NY (2×10^7 parasitized erythrocytes) was inoculated intravenously (iv) in MF1 mice supplied by the Biological Services Unit, The University of Manchester, U.K. Mice were housed in groups in plastic cages (length 38 cm × width 22 cm × height 11 cm) at room temperature (19−22 °C) on a 12 h light (08:00 to 20:00) and 12 h dark (20:00 to 08:00) cycle with unlimited access to food (CRM feeding pellets, SDS) and water. Experiments were licensed under the Animals (Scientific Procedures) Act 1986. In compliance with the conditions of the license, infected mice were humanely killed when humane endpoints were reached. Parasitemia was measured by counting Leishman-positive cells 72 h following infection using tail blood smears stained with Leishman's reagent

(Sigma Chemical Co.), 2 mg/mL of methanol. Parasitemia was calculated as the mean percentage ± SEM of erythrocytes containing Leishman-positive bodies for groups of four to eight mice for each dose tested. Drugs were delivered by the subcutaneous (sc, five injections over 72 h), intraperitoneal (ip, five injections over 72 h), or oral (drinking water, continuously available) route using delivery vehicles based on either olive oil or water as described in Results and Discussion. An appropriate number of dose levels (two through eight) were investigated for each compound to determine the dose of drug (ID_{50}) required to inhibit parasitemia by 50% compared with parasitemia in concurrent vehicle-treated mice.[5]

(b) In Vitro. Synchronized *P. falciparum* strain K1 parasites in mostly ring stage with a parasitemia of 1.0% were cultured in RPMI 1640 medium supplemented with 25 mM HEPES buffer, pH 7.4, 32 mM $NaHCO_3$ and the drug at various concentrations (stock drug solution was dissolved in 100% DMSO, and the final concentration of DMSO in parasite culture never exceeded 0.01%) for 24 h at 37 °C under 17% O_2, 3% CO_2, and 80% N_2, followed by a further incubation of 18−24 h in the presence of [^{3}H]hypoxanthine. Parasites were then harvested onto glass filter disks, and radioactivity incorporated into nucleic acids was measured using a liquid scintillation counter.[40]

Hemin−Drug Binding Experiments in Aqueous DMSO. Solutions of hemin and of various antimalarials ($(0-5) \times 10^{-5}$ M) at an apparent pH of 7.4 (HEPES buffer) were mixed in the wells of a 96-well microtiter plate (Cliniplate, Dynex Labsystems, Basingstoke, U.K.) and incubated at room temperature for 30 min before the absorbance of the solution was measured using a microtiter plate reader (Multiskan Ascent, Dynex Labsystems). The instrument was fitted with a 405 nm filter, and plates were automatically shaken for 10 s before the absorbances of the individual wells were rapidly determined. The plate reader was computer-controlled using Dynex Labsystems' Ascent software.

MS Investigation of Hemin-Binding Studies. The binding of chloroquine and of metaquine with hemin was studied using positive-ion electrospray mass spectroscopy (PI-ESMS) in LockSpray mode. An approximately 15×10^{-6} M solution of hemin was prepared in methanol, and this was infused at a rate of 10 μL min^{-1} into the mass spectrometer (LCT-TOF MS, Micromass Limited, Manchester, U.K.). The spectrometer was operated using factory-standard settings modified as follows: extraction cone = 1 V; sample cone = 30 V, RF lens = 400 V; ionization potential 3000 V; pusher time = 60 ms; desolvation temperature = 150 °C; source temperature = 100°C.[17g,24] Subsequently, a 1:1 adduct was prepared by constant mechanical agitation of hemin chloride and metaquine dihydrochloride using a mortar and pestle for 30 min. This adduct was dissolved in methanol and analyzed by HRMS electrospray as described above.

Acknowledgment. P.W. is a Senior Research Scholar of the Thailand Research Fund. We thank the EPSRC for access to the Cambridge Crystallographic Database[41] and Brian Robinson for the gift of *P. berghei* NY. Technical support was provided by Nicola Dempster, Giles Edwards, Ali Al-Rehawi, and Leslie Suttcliffe.

Supporting Information Available: Detailed depiction of drug−receptor interaction, mass spectra, and X-ray crystallographic data. This material is available free of charge via the Internet at http://pubs.acs.org.

References

(1) (a) Trape, J. F. The Public Health Impact of Chloroquine Resistance in Africa. *Am. J. Trop. Med. Hyg.* **2001**, *64*, 12−17. (b) Egan, T. J.; Hunter, R.; Kaschula, C. H.; Marques, H. M.; Mavuso, W. W. Towards the Rational Design of Antimalarial Drugs. *S. Afr. J. Sci.* **1998**, *94*, 277−278. (c) Foley, M.; Tilley, L. Quinoline Antimalarials: Mechanisms of Action and Resistance in *Plasmodia*: Prospects for New Agents. *Pharmacol. Ther.* **1998**, *79*, 55−87. (d) Ridley, R. G. Medical Need, Scientific Opportunity and the Drive for Antimalarial Drugs. *Nature* **2002**, *415*, 686−693.

(2) (a) Omodeo-Sale, F.; Monti, D.; Olliaro, P.; Taramelli, D. Prooxidant Activity of Beta-Hematin (Synthetic Malaria Pigment) in Arachidonic Acid Micelles and Phospholipid Large Unilamellar Vesicles. *Biochem. Pharmacol.* **2001**, *61*, 999−1009. (b) Pagola, S.; Stephens, P. W.; Bohle, D. S.; Kosar, A. D.; Madsen, S. K. The Structure of Malaria Pigment Beta-Haematin. *Nature* **2000**, *404*, 307−310. (c) Francis, S. E.; Sullivan, D. J., Jr.; Goldberg D. E. Hemoglobin Metabolism in the Malaria Parasite *Plasmodium falciparum*. *Annu. Rev. Microbiol.* **1997**, *51*, 97−123. (d) Tolosano, E.; Altruda, F. Hemopexin: Structure, Function, and Regulation. *DNA Cell Biol.* **2002**, *21*, 297−306.

(3) (a) Ridley, R. G. Haemoglobin Degradation and Haem Polymerization as Antimalarial Drug Targets. *J. Pharm. Pharmacol.* **1997**, *49*, 43−48. Ridley, R. G.; Hudson, A. T. Quinoline Antimalarials. *Expert Opin. Ther. Pat.* **1998**, *8*, 121−136. (b) Bray, P. G.; Mungthin, M.; Ridley, R. G.; Ward, S. A. Access to Hematin: The Basis of Chloroquine Resistance. *Mol. Pharmacol.* **1998**, *54*, 170−179. (c) Egan, T. J.; Marques, H. M. The Role of Haem in the Activity of Chloroquine and Related Antimalarial Drugs. *Coord. Chem. Rev.* **1999**, *192*, 493−517. (d) Egan, T. J.; Hunter, R.; Kaschula, C. H.; Marques, H. M.; Misplon, A.; Walden J. Structure−Function Relationships in Aminoquinolines: Effect of Amino and Chloro Groups on Quinoline−Hematin Complex Formation, Inhibition of Beta-Hematin Formation, and Antiplasmodial Activity. *J. Med. Chem.* **2000**, *43*, 283−291. (e) Egan, T. J.; Mavuso, W. W.; Ncokazi, K. K. The Mechanism of Beta-Hematin Formation in Acetate Solution, Parallels between Hemozoin Formation and Biomineralization Processes. *Biochemistry* **2001**, *40*, 204−213. (f) Egan, T. J. Quinoline Antimalarials. *Expert Opin. Ther. Pat.* **2001**, *11*, 185−209. (g) Pandey, A. V.; Bisht, H.; Babbarwal, V. K.; Srivastava, J.; Pandey, K. C.; Chauhan, V. S. Mechanism of Malarial Haem Detoxification Inhibition by Chloroquine. *Biochem. J.* **2001**, *355*, 333−338. (h) Ziegler, J.; Linck, R.; Wright, D. W. Heme Aggregation Inhibitors: Antimalarial Drugs Targeting an Essential Biomineralization Process. *Curr. Med. Chem.* **2001**, *8*, 171−189. (i) Egan, T. J. Physico-Chemical Aspects of Hemozoin (Malaria Pigment) Structure and Formation. *J. Inorg. Biochem.* **2002**, *91*, 19−26.

(4) Kaschula, C. H.; Egan, T. J.; Hunter, R.; Basilico, N.; Parapini, S.; Taramelli, D.; Pasini, E.; Monti, D. Structure−Activity Relationships in 4-Aminoquinoline Antiplasmodials. The Role of the Group at the 7-Position. *J. Med. Chem.* **2002**, *45*, 3531−3539.

(5) (a) Ismail, F. M. D.; Dascombe, M. J.; Carr P.; Merette S. A. M.; Rouault, P. Novel Aryl-*bis*-quinolines with Antimalarial Activity *in-vivo*. *J. Pharm. Pharmacol.* **1996**, *50*, 483−492. (b) The virulence of *Plasmodia* depends partly on the strain of parasite and partly on the host. In this study, *Plasmodium berghei* strains (N/13/1A/4/203 and NY) that caused the death of untreated mice usually on day 5 of infection were used. Nahrevanian, H.; Dascombe M. J. Nitric Oxide and Reactive Nitrogen Intermediates during Lethal and Nonlethal Strains of Murine Malaria. *Parasite Immunol.* **2002**, *23*, 491−501.

(6) Ismail, F. M. D.; Dascombe, M. J.; Carr, P.; North, S. E. An Exploration of the Structure−Activity Relationships of 4-Aminoquinolines: Novel Antimalarials with Activity in-Vivo. *J. Pharm Pharmacol.* **1998**, *48*, 841−850.

(7) (a) McKie, J. H.; Douglas, K. T.; Chan, C.; Roser, S. A.; Yates, R.; Read, M.; Hyde, J. E.; Dascombe, M. J.; Yuthavong, Y.; Sirawaraporn, W. Rational Drug Design Approach for Overcoming Drug Resistance: Application to Pyrimethamine Resistance in Malaria. *J. Med. Chem.* **1998**, *41*, 1367−1370. (b) Drew, M. G. B.; Metcalfe, J.; Ismail, F. M. D. *J. Mol. Struct.: THEOCHEM* **2004**, *711*, 95−105.

(8) Frearson, M. J.; Bhatt, R.; Carr, P.; Ismail, F. M. D. Electron Impact Induced Elimination of HNO_2 from Trifluralin−Phenylenediamine Dimers−An Ortho Effect Resulting from a pi−pi Interaction Persisting into the Vapour Phase. *Rapid Commun. Mass Spectrom.* **1997**, *11*, 201−205.

(9) (a) Alizadeh-Shekalgourabi, S.; Dascombe, M. J.; Drew, M. G. B.; Ismail, F. M. D. Unpublished study. (b) Dascombe, M. J.; Ismail, F. M. D.; Carr, P.; Alizadeh Shekalgourabi, S.; Moule, W. A.; Evans, P. G. Exploration of Structure Activity Relationships between *Monomeric and Dimeric* 4-Aminoquinolines; Synthesis, Pharmacology and Molecular Modelling of Novel Antimalarials with Activity in vivo. Unpublished study. (c) Ismail, F. M. D.; Dascombe, M. J.; Wilairat, P.; Carr, P.; Sutcliffe, L. J.; Auparakkitanon, S.; Alizadeh Shekalgourabi, S.; Moule, W. A.; Evans, P. G. Synthesis, Pharmacology and Molecular Modelling of Bisquinolines. Unpublished study.

(10) Apex-3D was a rule-based QSAR program developed by Biosym Technologies in conjunction with V. E. Golender and A. B. Rozenblit. The program is no longer available; therefore, Figure 2 was rerendered using Cerius^2 for clarity. For leading references for generating pharmacophores using the APEX package, see the following: (a) Pandya, T.; Pandey, S. K.; Tiwari, M.; Chaturvedi, S. C.; Saxena, A. K. 3-D QSAR Studies of Triazolinone Based Balanced AT(1)/AT(2) Receptor Antagonists. *Bioorg. Med. Chem.* **2001**, *9*, 291−300. (b) Vajragupta, O.; Boonchoong, P.; Wongkrajang, Y. Comparative Quantitative Structure−Activity Study of Radical Scavengers. *Bioorg. Med. Chem.* **2000**, *8*, 2617−2628. (c) Talele, T. T.; Kulkarni, S. S.; Kulkarni, V. M. Development of Pharmacophore Alignment Models as Input for Comparative Molecular Field Analysis of a Diverse Set of Azole Antifungal Agents. *J. Chem. Inf. Comput. Sci*. **1999**, *39*, 958−966. (d) Bessis, A. S.; Jullian, N.; Coudert, E.; Pin, J. P.; Acher, F. Extended Glutamate Activates Metabotropic Receptor Types 1, 2 and 4: Selective Features at mGluR4 Binding Site. *Neuropharmacology* **1999**, *38*, 1543−1551. (e) Jullian, N.; Brabet, I.; Pin, J. P.; Acher, F. C. Agonist Selectivity of mGluR1 and mGluR2 Metabotropic Receptors: A Different Environment but Similar Recognition of an Extended Glutamate Conformation. *J. Med. Chem*. **1999**, *42*, 1546−1555. (f) Talele, T. T.; Kulkarni, V. M. Three-Dimensional Quantitative Structure−Activity Relationship (QSAR) and Receptor Mapping of Cytochrome P-450 (14 alpha DM) Inhibiting Azole Antifungal Agents. *J. Chem. Inf. Comput. Sci*. **1999**, *39*, 958−966. (g) Bremner, J. B.; Coban, B.; Griffith, R. Pharmacophore Development for Antagonists at Alpha(1) Adrenergic Receptor Subtypes. *J. Comput.-Aided Mol. Des.* **1996**, *10*, 545−557. (h) Hariprasad, V.; Kulkarni, V. M. A Proposed Common Spatial Pharmacophore and the Corresponding Active Conformations of Some Peptide Leukotriene Receptor Antagonists. *J. Comput.-Aided Mol Des.* **1996**, *10*, 284−292. (i) *Pharmacophore Perception, Development, and Use in Drug Design*; Guner, O. F., Ed.; International University Line: La Jolla, CA, 2000.

(11) Go, M. L.; Koh, H. L.; Ngiam, T. L.; Phillipson, J. D.; Kirby, G. C.; O'Neill, M. J.; Warhurst, D. C. Synthesis and in Vitro Antimalarial Activity of Some Indolo[3,2-*C*]quinolines. *Eur. J. Med. Chem*. **1992**, *27*, 391−394.

(12) Alizadeh-Shekalgourabi, S.; Dascombe, M. J.; Drew, M. G. B.; Ismail, F. M. D. Pharmacology, Spectroscopy and Molecular Modelling of Ro-47-7737. Presented at the Biological and Medicinal Chemistry Sector (BMCS) of the Royal Society of Chemistry (RSC), 11th Symposium of Medicinal Chemistry, Fielder Centre, Hatfield, U.K., 2000; Poster Presentation.

(13) (a) Vennerstrom, J. L.; Ellis, W. Y.; Ager, A. L.; Andersen, S. L.; Gerena, L.; Milhous, W. K. Bisquinolines. 1. *N*,*N*-Bis(7-chloroquinolin-4-yl)alkanediamines with Potential against Chloroquine-Resistant Malaria. *J. Med. Chem.* **1992**, *35*, 2129−2134. (b) Ridley, R. G.; Matile, H.; Jaquet, C.; Dorn, A.; Hofheinz, W.; Leupin, W.; Masciadri, R.; Theil, F.-P. Richter, W. F.; Girometta, M.-A.; Guenzi, A.; Urwyler, H.; Gocke, E.; Potthast, J.-M.; Csato, M.; Thomas, A.; Peters, W. Antimalarial Activity of the Bisquinoline *trans*-N^1,N^2-Bis(7-chloroquinolin-4-yl)cyclohexane-1,2-diamine: Comparison of Two Stereoisomers and Detailed Evaluation of the *S*,*S* Enantiomer, Ro 47-7737. *Antimicrob. Agents Chemother.* **1997**, *41*, 677−686. (c) Vennerstrom, J. L.; Ager, A. L.; Dorn, A.; Andersen, S. L.; Gerena, L.; Ridley, R. G.; Milhous, W. K. Bisquinolines. 2. Antimalarial *N*,*N*-Bis(7-chloroquinolin-4-yl)heteroalkanediamines. *J. Med Chem.* **2002**, *41*, 4360−4364. (d) Karle, J. M.; Bhattacharjee, A. K.; Vennerstrom, J. L. Crystal Structure of the Potent Bisquinoline Antimalarial Agent (±)-*trans*-*N*-^{1},*N*-^{2}-Bis(7-chloroquinolin-4-yl)cyclohexane-1,2-diamine Dimethanesulfonate Salt Hydrate in Relation to Its Biological Properties. *J. Chem. Crystallogr.* **2002**, *32*, 133−139. (e) Ismail, F. M. D.; Drew, M. G. B.; Dascombe, M. J.; Clark, I. P.; Parker, A. W. Unravelling the mechanism of 4-aminoquinoline antimalarial action. CCLRC Annual Report, Central Laser Facility, Chilton, U.K., 2004; pp 119−120 (http://www.clf.rl.ac.uk/Reports/2003-2004/pdf/54.pdf).

(14) (a) CrossFireBeilstein: see http://www.beilstein.com/splashscreen.shtml, MDL Information Systems GmbH. (b) Heme binding proteins in *Plasmodium* were unknown when this study was initiated; however, see the following: Choi, C. Y. H.; Cerda, J. F.; Chu, H. A.; Babcock, G. T.; Marletta, M. A. Spectroscopic Characterization of the Heme-Binding Sites in *Plasmodium falciparum* Histidine-Rich Protein 2. *Biochemistry* **1999**, *38*, 16916−16924.

(15) (a) Cerius^2 software package is fully parametrized for Fe and has since replaced Macromodel software package in our investigations: Drew, M. G. B.; Male, V.; Dascombe, M. J.; Ismail, F. M. D. Unpublished studies. (b) Endocyclic quinoline to 4-aminoquinoline distances in heme: N1−N1, 6.877 Å; N1−N12, 4.215 and 7.165 Å; N12−N12, 4.885 Å (see Figure 4 for numbering system); Fe−O, 8.29−8.58 Å; N−N, 2.84 Å for cis and 4.11 Å for trans.

(16) (a) Frisch, M. J.; Trucks, G. W.; Schlegel, H. B.; Scuseria, G. E.; Robb, M. A.; Cheeseman, J. R.; Zakrzewski, V. G.; Montgomery, J. A., Jr.; Stratmann, R. E.; Burant, J. C.; Dapprich, S.; Millam, J. M.; Daniels, A. D.; Kudin, K. N.; Strain, M. C.; Farkas, O.; Tomasi, J.; Barone, V.; Cossi, M.; Cammi, R.; Mennucci, B.; Pomelli, C.; Adamo, C.; Clifford, S.; Ochterski, J.; Petersson, G. A.; Ayala, P. Y.; Cui, Q.; Morokuma, K.; Malick, D. K.; Rabuck, A. D.; Raghavachari, K.; Foresman, J. B.; Cioslowski, J.; Ortiz, J. V.; Stefanov, B. B.; Liu, G.; Liashenko, A.; Piskorz, P.; Komaromi, I.; Gomperts, R.; Martin, R. L.; Fox, D. J.; Keith, T.; Al-Laham, M. A.; Peng, C. Y.; Nanayakkara, A.; Gonzalez, C.; Challacombe, M.; Gill, P. M. W.; Johnson, B. G.; Chen, W.; Wong, M. W.; Andres, J. L.; Head-Gordon, M.; Replogle, E. S.; Pople, J. A. *Gaussian 98*; Gaussian, Inc.: Pittsburgh, PA, 1998. (b) Sheldrick, G. M. Phase Annealing in Shelx-90. Direct Methods for Larger Structures. *Acta Crystallogr.* **1990**, *A46*, 467−473. (c) Sheldrick, G. M. *Shelxl Program for Crystal Structure Refinement*; University of Gottingen: Gottingen, Germany, 1993.

(17) Various pharmacophores have been published, but these have relied on observations derived from testing rather than employing a pharmacophore-based approach. Activity of the corresponding a-(2-piperidylmethyl) derivatives conforms with the postulated triangle pharmacophore for antimalarial activity. (a) Chien, P.-L.; Cheng, C. C. Difference in Antimalarial Activity between Certain Amino Alcohol Diastereomers. *J. Med. Chem.* **1976**, *19*, 170−172. (b) Chien, P.-L.; Cheng C. C. Further Side-Chain Modification of Antimalarial Phenanthrene Amino Alcohols. *J. Med. Chem.* **1973**, *16*, 1093−1096. (c) Jefford, C. W.; Grigorov, M.; Weber, J.; Luthi, H. P.; Tronchet, J. M. J. Correlating the Molecular Electrostatic Potentials of Some Organic Peroxides with Their Antimalarial Activities. *J. Chem. Inf. Comput. Sci.* **2000**, *40*, 354−357. (d) Grigorov, M.; Weber, J.; Tronchet, J. M. J.; Jefford, C. W.; Milhous, W. K.; Maric, D. A QSAR Study of the Antimalarial Activity of Some Synthetic 1,2,4-Trioxanes. *J. Chem. Inf. Comput. Sci.* **1997**, *37*, 124−130. (e) Avery, M. A.; Alvim-Gaston, M.; Vroman, J. A.; Wu, B.; Ager, A.; Peters, W.; Robinson, B. L.; Charman, W. Structure−Activity Relationships of the Antimalarial Agent Artemisinin. 7. Direct Modification of (+)-Artemisinin and in Vivo Antimalarial Screening of New, Potential Preclinical Antimalarial Candidates. *J. Med. Chem.* **2002**, *45*, 4321−4335. (f) Avery, M. A.; Alvim-Gaston, M.; Rodrigues, C. R.; Barreiro, E. J.; Cohen, F. E.; Sabnis, Y. A.; Woolfrey, J. R. Structure−Activity Relationships of the Antimalarial Agent Artemisinin. 6. The Development of Predictive in Vitro Potency Models Using CoMFA and HQSAR Methodologies. *J. Med. Chem.* **2002**, *45*, 292−303. (g) Konig, G. M.; Wang, H.; Gurrath, M.; Wright, A. D.; Kocak, G.; Neumann, G.; Loria, P.; Foley, M.; Tilley, L. Inhibition of Heme Detoxification Processes Underlies the Antimalarial Activity of Terpene Isonitrile Compounds from Marine Sponges. *J. Med. Chem.* **2001**, *44*, 873−885. (h) Girones, X.; Gallegos, A.; Carbo-Dorca, R. Modeling Antimalarial Activity: Application of Kinetic Energy Density Quantum Similarity Measures as Descriptors in QSAR. *J. Chem. Inf. Comput. Sci.* **2000**, *40*, 1400−1407. (i) Livingstone, D. J. The Characterization of Chemical Structures Using Molecular Properties. A Survey. *J. Chem. Inf. Comput. Sci.* **2000**, *40*, 195−209. (j) Alzeer, J.; Chollet, J.; Heinze-Krauss, I.; Hubschwerlen, C.; Matile, H.; Ridley, R. G. Phenyl β-Methoxyacrylates: A New Antimalarial Pharmacophore. *J. Med. Chem.* **2000**, *43*, 560−568. (k) Ghose, A. K.; Viswanadhan, V. N.; Wendoloski, J. J. A Knowledge-Based Approach in Designing Combinatorial or Medicinal Chemistry Libraries for Drug Discovery. 1. A Qualitative and Quantitative Characterization of Known Drug Databases. *J. Comb. Chem.* **1999**, *1*, 55−68. (l) Hibert, M. F.; Gittos, M. W.; Middlemiss, D. N.; Mir, A. K.; Fozard, J. R. Graphics Computer-Aided Receptor Mapping as a Predictive Tool for Drug Design: Development of Potent, Selective, and Stereospecific Ligands for the 5-HT1A Receptor. *J. Med. Chem.* **1988**, *31*, 1087−1093. (m) Brint, A. T.; Willett, P. Algorithms for the Identification of Three-Dimensional Maximal Common Substructures. *J. Chem. Inf. Comput. Sci.* **1987**, *27*, 152−158. (n) Martin, Y. C. A Practitioner's Perspective of the Role of Quantitative Structure−Activity Analysis in Medicinal Chemistry. *J. Med. Chem.* **1981**, *24*, 229−237. (o) For a recent study using catalyst to define a resistance reversal pharmacophore, see the following: Bhattacharjee, A. K.; Kyle, D. E.; Vennerstrom, J. L.; Milhous, W. K. A 3D QSAR Pharmacophore Model and Quantum Chemical Structure−Activity Analysis of Chloroquine (CQ)-Resistance Reversal. *J. Chem. Inf. Comput. Sci.* **2002**, *42*, 1212−1220.

(18) Ismail, F. M. D.; Dascombe, M. J. The Rational Design, Synthesis and Pharmacological Evaluation of Novel Metazaquines. Presented at the New Medicines for Malaria Venture Expert Advisory Committee Meeting, WHO, Geneva, Switzerland, 1999 (Invited Presentation).

(19) (a) Lee, P.; Ye, Z.; Vandyke, K.; Kirk, R. G. X-ray Microanalysis of *Plasmodium falciparum* and Infected Red Blood Cells: Effects of Qinghaosu and Chloroquine on Potassium, Sodium, and pHosphorus Composition. *Am. J. Trop. Med. Hyg*. **1988**, *39*, 157−165. (b) Kirk, K. Membrane Transport in the Malaria-Infected Erythrocyte. *Physiol. Rev.* **2001**, *81*, 495−537.

(20) Boffi, A.; Das, T. K.; Longol, S. L.; Spagnuolo, C.; Rousseau, D. L. Pentacoordinate Hemin Derivatives in Sodium Dodecyl Sulfate Micelles: Model Systems for the Assignment of the Fifth Ligand in Ferric Heme Proteins. *Biophys. J.* **1999**, *77*, 1143−1149.

(21) Constantinindis, I.; Saterlee, J. D. UV−Visible and Carbon NMR Studies of Chloroquine Binding to Urohemin I Chloride and Uroporphyrin I in Aqueous Solutions. *J. Am. Chem. Soc.* **1988**, *110*, 4391−4395.

(22) (a) Jorgensen, W. L.; Severance, D. L. Aromatic−Aromatic Interactions: Free Energy Profiles for the Benzene Dimer in Water, Chloroform, and lIquid Benzene. *J. Am. Chem. Soc.* **1990**, *112*, 4768−4774. (b) Hunter, C. A.; Sanders, J. K. M. The nature of $\pi-\pi$ interactions. *J. Am. Chem. Soc.* **1990**, *112*, 5525−5534.

(23) Shelnutt, J. A.; Song, X.-Z.; Ma, J.-G.; Jia, S.-L.; Jentzen, W.; Medforth, C. J. Nonplanar Porphyrins and Their Significance in Proteins. *Chem. Soc. Rev*. **1998**, *27*, 31−41.

(24) (a) Janiak, C. A Critical Account on $\pi-\pi$ Stacking in Metal Complexes with Aromatic Nitrogen-containing Ligands. *J. Chem. Soc., Dalton Trans.* **2000**, 3885−3896. Note "below face" binding of metaquine to heme, in addition to "above face" binding, was detected, but "below face" binding had a slightly higher energy and exhibited $\pi-\pi$ interactions with the underside of the heme molecule. (b) Note the incorrect transposition of methyl and vinyl groups in modelled heme by the following: O'Neill, P. M.; Willock, D. J.; Hawley, S. R.; Bray, P. G.; Storr, R. C.; Ward, S. A.; Park, B. K. Synthesis, Antimalarial Activity, and Molecular Modeling of Tebuquine Analogues. *J. Med. Chem*. **1997**, *40*, 437−448. (c) It is interesting to speculate why the automated docking program did not provide the lowest energy conformation. It seems likely that this is due to the fact that the heme was included as planar to obtain the initial models for docking. After metaquine was docked with hematin in a particular geometry, the exact nature of the ruffling of the heme could be established, but this could not be predicted in advance. Perhaps automatic docking would have been more successful if several different ruffled hemes were considered. (d) Note the solution-state studies of antimalarial complexes with hematin: Leed, A.; DuBay, K.; Ursos, L. M. B.; Sears, D.; de Dios, A. C.; Roepe, P. D. Solution Structures of Antimalarial Drug−Heme Complexes. *Biochemistry* **2002**, *41*, 10245−10255. Importantly in this latter study, modelled structures exhibiting "planarity violations" were discarded before correlations with NMR data were sought. This process could bias the data set toward structures that are predominately π-stacked.

(25) Levan, K. R.; Strouse, C. E. *Am. Crystallogr. Assoc., Ser. 2* **1982**, *10*, 30 (Deposition in Cambridge Crystallography Data Centre, Ref BIXZAJ).

(26) Thomson, P. E.; Werbel, L. M. *Antimalarial Agents: Chemistry and Pharmacology*; Academic Press: New York, 1972.

(27) Kurosawa, Y.; Dorn, A.; Kitsuji-Shirane, M.; Shimada, H.; Satoh, T.; Matile, H.; Hofheinz, W.; Masciadri, R.; Kansy, M.; Ridley, R. G. Hematin Polymerization Assay as a High-Throughput Screen for Identification of New Antimalarial Pharmacophores. *Antimicrob. Agents. Chemother*. **2000**, *44*, 2638−2644.

(28) (a) Egan T. J.; Hempelmann, E.; Mavuso, W. W. Characterisation of Synthetic Beta-Haematin and Effects of the Antimalarial Drugs Quinidine, Halofantrine, Desbutylhalofantrine and Mefloquine on Its Formation *J. Inorg. Biochem*. **1999**, *73*, 101−107. (b) Egan, T. J.; Mavuso, W. W.; Ross, D. C.; Marques, H. M. Thermodynamic Factors Controlling the Interaction of Quinoline Antimalarial Drugs with Ferriprotoporphyrin IX. *J. Inorg. Biochem*. **1997**, *68*, 137−145. (c) Egan, T. J. Physicochemical aspects of hemozoin (malaria pigment) structure and formation. *J. Inorg Biochem*. **2002**, *91*, 19−26. (d) Egan, T. J.; Ncokazi, K. K. Effects of Solvent Composition and Ionic Strength on the Interaction of Quinoline Antimalarials with Ferriprotoporphyrin IX. *J. Inorg. Biochem.* **2004**, *98*, 144−152. (e) Under normal laboratory atmospheric conditions, metaquine in this system tends to precipitate out of solution at values close to those in parasitic vacuoles (e.g., pH 5.0). (f) Importantly, aminoquinolines, 9-aminoarylacridines, and benznaphthyridines all formed complexes with hemin, suggesting that they shared a common mode of quinoline-like action (Brown, C.; Dascombe, M. J.; Drew, M. G. B.; Dyas, A. M.; Ismail, F. M. D.; Lloyd, M.; Morris, H. Unpublished study). (g) Chou, A. C.; Chevli, R.; Fitch, C. D. Ferriprotoporphyrin IX Fulfills the Criteria for Identification as the Chloroquine Receptor of Malaria Parasites. *Biochemistry* **1980**, *19*, 1543−1549. (h) The reason for this phenomenon remains uncertain, but we have observed a gel to sol phase transition at this temperature in certain types of metaquine dosage forms. This phenomenon is under current investigation. (i) Buller, R.; Peterson, M. L.; Almarsson, O.; Leiserowitz, L. Quinoline Binding Site on Malaria Pigment Crystal: A Rational Pathway for Antimalaria Drug Design. *Cryst. Growth Des.* **2002**, *2*, 553−562. Note that in this study chloroquine was incorrectly modelled and docked, while protonated on the endocyclic nitrogen (see their Figure 6) rather than the endocyclic quinoline nitrogen found in solution-state NMR studies. The report by Buller et al. also contradicts the site of quinoline protonation detailed in the solid-state X-ray data reported by Vennerstrom et al.[13d]

(29) Warhurst, D. C. Antimalarial Interaction with Ferriprotoporphyrin-IX Monomer and Its Relationship to Activity of the Blood Schizontocides. *Ann. Trop. Med. Parasitol.* **1987**, *81*, 65−67.

(30) Vippagunta, S. R.; Dorn, A.; Matile, H.; Bhattacharjee, A. K.; Karle, J. M.; Ellis, W. Y.; Ridley, R. G.; Vennerstrom, J. L. Structural Specificity of Chloroquine−Hematin Binding Related to Inhibition of Hematin Polymerization and Parasite Growth. *J. Med. Chem*. **1999**, *42*, 4630−4639. See the note at the end of ref 16 in the Vippagunta publication.

(31) (a) The designation SN identifies a compound in the following monograph: *A Survey of Antimalarial Drugs 1941−1945*; Wiselogle, F. Y., Ed.; Edwards: Ann Arbor, MI, 1946. (b) Burckhalter, J. H.; Tendick, F. H.; Jones, E. M.; Jones, P. A.; Holcomb, W. F.; Rawlins A. L. Aminoalkylphenols as Antimalarials. II. (Heterocyclic-amino)-α-amino-*o*-cresols. The Synthesis of Camoquin. *J. Am. Chem. Soc.* **1948**, *70*, 1363−1373.

(32) Wolff, J. C.; Thomson, L. A.; Eckers, C. Identification of the "Wrong" Active Pharmaceutical Ingredient in Counterfeit in Halfan Drug Product Using Accurate Mass Electrospray Ionization Mass Spectrometry, Accurate Mass Tandem Mass Spectrometry and Liquid Chromatography/Mass Spectrometry. *Rapid Commun. Mass Spectrom*. **2003**, *17*, 215−221.

(33) Leed, A.; DuBay, K.; Ursos, L. M. B.; Sears, D.; deDios, A. C.; Roepe, P. D. Solution Structures of Antimalarial Drug−Heme Complexes. *Biochemistry* **2002**, *41*, 10245−10255.

(34) deDios, A. C.; Tycko, R.; Ursos, L. M. B.; Roepe, P. D. NMR Studies of Chloroquine−Ferriprotoporphyrin IX Complex. *J. Phys. Chem.* **2003**, *107*, 5821−5825.

(35) (a) Dorn, A.; Vippagunta, S. R.; Matile, H.; Jaquet, C.; Vennerstrom, J. L.; Ridley, R. G. An Assessment of Drug−Hematin Binding as a Mechanism for Inhibition of Hematin Polymerisation by Quinoline Antimalarials. *Biochem. Pharmacol*. **1998**, *55*, 727−736. (b) Cheruku, S. R.; Maiti, S.; Dorn, A.; Scorneaux, B.; Bhattacharjee, A. K.; Ellis, W. Y.; Vennerstrom, J. L. Carbon Isosteres of the 4-Aminopyridine Substructure of Chloroquine: Effects on pK_a, Hematin Binding, Inhibition of Hemozoin Formation, and Parasite Growth. *J. Med. Chem.* **2003**, *46*, 3166−3169.

(36) Monti, D.; Vodopivec, B.; Basilico, N.; Olliaro, P.; Taramelli, D. A Novel Endogenous Antimalarial: Fe(II)-Protoporphyrin IX α-(Heme) Inhibits Hematin Polymerization to β-Hematin (Malaria Pigment) and Kills Malaria Parasites. *Biochemistry* **1999**, *38*, 8858−8863.

(37) Koenig, D. F. The Structure of α-Chlorohemin. *Acta Crystallogr.* **1965**, *18*, 663−673.

(38) Cohen, I. A. Dimeric Nature of Hemin Hydroxides. *J. Am. Chem. Soc.* **1969**, *91*, 1980−1983.

(39) Alben, J. O.; Fuchsman, W. H.; Beaudreau, C. A.; Caughey, W. S. Substituted Deuteroporphyrins. III. Iron(II) derivatives. Reactions with oxygen and preparations from chloro- and methoxohemins. *Biochemistry* **1968**, *7*, 624−635.

(40) (a) Desjardins, R. E.; Canfield, C. J.; Haynes, J. D.; Chulay, J. C. Quantitative Assessment of Antimalarial Activity in Vitro by a Semi-automated Microdilution Technique. *Antimicrob. Agents Chemother.* **1979**, *16*, 710−718. (b) Chavalitshewinkoon-Petmitr, P.; Pongvilairat, G.; Auparakkitanon, S.; Wilairat, P. Gametocidal Activity of Pyronaridine and DNA Topoisomerase II Inhibitors against Multidrug-Resistant *Plasmodium falciparum* in vitro. *Parasitol. Int.* **2000**, *48*, 275−280. (c) PfK1 strain is both chloroquine and pyrimethamine resistant: Thaithong S.; Beale, G. H.; Chutmongkonkul, M. Susceptibility of *Plasmodium falciparum* to Five Drugs: An in Vitro Study of Isolates Mainly from Thailand. *Trans. R. Soc. Trop. Med. Hyg.* **1983**, *77*, 228−231.

(41) Fletcher, D. A.; McMeeking, R. F.; Parkin, D. The United Kingdom Chemical Database Service. *J. Chem. Inf. Comput. Sci.* **1996**, *36*, 746−749.

(42) Baerends, E. J.; Berces, A.; Bo, C.; Boerrigter, P. M.; Cavallo, L.; Deng, L.; Dickson, R. M.;.Ellis, D. E.; Fan, L.; Fisher, T. H.; Fonseca-Guerra, C.; van Gisbergen, S. J. A.; Groeneveld, J. A.; Gritsenko, O. V.; Harris, F. E.; van Hoek, D.; Jacobson, P. H.; van Kessel, G.; Kootstra, F.; van Lenthe, E.; Osinga, V. E.; Philipson, P. H. T.; Post, D.; Pye, C. C.; Ravenek, W.; Ros, P.; Schipper, P. R. T.; Schreckenback, G.; Snijders, J. G.; Sola, M.; Swerhone, D.; te Velde, G.; Vernooijs, P.; Versluis, L.; Visser, O.; van Wezenbeek, E.; Wiesenekker, G.; Wolff, S. K.; Woo, T.; Ziegler, T. *ADF2000 Program*; SCM Inc., Theoretical Chemistry, Vrije Universiteit: Amsterdam, The Netherlands, 2000.

(43) Vosko, S. H.; Wilk, L.; Nusair, M. Accurate Spin-dependent Electron Liquid Correlation Energies for Local Spin Density Calculations: A Critical Analysis. *Can. J. Phys.* **1980**, *58*, 1200−1211.
(44) Becke, A. D. Correlation-Energy of an Inhomogeneous Electron-Gas. A Coordinate-Space Model. *J. Chem. Phys.* **1988**, *88*, 1053−1062.
(45) (a) Perdew, J. P., Density-Functional Approximation for the Correlation-Energy of the Inhomogeneous Electron-Gas. *Phys. Rev.* **1986**, *B33*, 8822−8824. (b) Perdew, J. P. Correction. *Phys.* Rev. **1986**, *B34*, 7406.

JM0408013